

Journal of Engineering Science and Technology
Vol. 13, No. 6 (2018) 1782 - 1792
© School of Engineering, Taylor's University

SIMULATION OF HYBRID LASER-TIG WELDING PROCESS USING FEA

HARINADH VEMANABOINA^{1,*}, G. EDISON²,
SURESH AKELLA³, RAMESH KUMAR BUDDU⁴

¹Associate Professor, NNR Group of Institutions, Hyderabad, 500088, India

²Professor, SMEC, VIT University, Vellore, Tamilnadu, India

³Professor, Sreyas Institute of Engineering & Technology,
Nagole, Hyderabad-500068, India

⁴Scientist-F, Institute for Plasma Research, FRMDC Division,
Bhat, Gandhinagar-382428, Gujarat, India

*Corresponding Author: harinadh.vh@gmail.com

Abstract

Hybrid welding technology has wide advantages in welding to improve speed, weldability of special materials, increasing depth of weld. Less defects of the weld, less bead widths, less temperature, less distortion and less residual stresses are seen. In this study, a three-dimensional Finite Element Model is developed for butt joints for SS316L. The heat flux models of double ellipsoidal surface heat flux of TIG process and lateral heat to the thickness face of laser process are used to model combined TIG and Laser welding processes for simulating. Total heat is distributed as surface heat flux and lateral heat flux, which can be incorporated in modelling with the proportion for Hybrid laser-TIG welding process. The transient thermal analysis, with thermally dependent properties, is performed to achieve the temperature distribution during the process; later, it is used to apply for the mechanical analysis of distortion and stresses. Uniform distortion along the weld with edge deformations is found. Residual stresses will maintain structural integrity with minimum 1.3 factor of safety. In this study, to save computing time, symmetric conditions were used for analyzing only half the product.

Keywords: ANSYS, Heat flux, Hybrid laser-TIG welding, Residual stress temperatures.

1. Introduction

TIG (Tungsten inert gas) welding process is one of the well-established metal joining methods accepted in industries for its high production rates, reliability and

Nomenclatures

c	Specific heat, J/kg k
H	Convective heat transfer coefficient, W/m ² K
K_m	Thermal conductivity, W/m ² K
Q	Energy input rate, W
q_L	Heat flux of laser process, W/m ²
q_T	Heat flux of TIG process, W/m ²
T	Temperature, K

Greek Symbols

ρ	Material density, kg/m ³
ε	Emissivity

Abbreviations

APDL	ANSYS Parametric Design Language
FEA	Finite Element Analysis
FZ	Fusion Zone
HAZ	Heat Affected Zone
TIG	Tungsten Arc Gas Welding

not having to change electrodes frequently. Shah and Madhvani [1] have given a review of this process and referred to many sources including Sándor and Dobranszky [2]. The heat in the TIG process is due to the transfer to the surface of the metals to be joined. The heat transfer process is a combination of a surface heat conduction and convection process. TIG process is having the limitation of the thickness of weld penetration, speed for automated process and providing flux. The conduction process of heat transfer is slow and the metal joining process had a boost with laser welding process.

Laser optical beams travelling and focussing on to the joining metal can form very high-intensity range from 100 to 1000 W/mm². The fusion and heat-affected zone being very narrow the welding bead formed are clean and neat with not requiring electrodes or flux and not leaving slag or splatter. The high-intensity heat melts the metal surface and forms fumes; plasma phase of metal is formed on the top surface and forms a keyhole in between the metals to be joined. The laser beam penetrates the top plasma enters the keyhole and gets entrapped. By convection of the molten metal in the keyhole and by conduction the heat of laser laterally enters the metal. As the laser travels further down the weld path, the molten metal solidifies to provide the weld joint. You et al. [3] gave a brief of this process and gave details of six sensors, which may be used for monitoring and controlling welding process, evaluating the weld and for providing preventive measures. With all the benefits associated again, the limitation happens to be the depth of the keyhole formation; and, hence the thickness of the weld can be obtained.

To obtain the combined benefits of TIG and laser processes a hybrid or combined welding process evolved. Here the TIG process of surface heating preludes causing preheating of metals and followed by the laser beam process of forming and penetrating the keyhole welding. Figure 1 shows the principle of the hybrid laser-TIG welding process. Hybrid welding modelling, analysis and simulation were also formulated by scientists and technocrats Belhadj et al. [4]. In

hybrid laser welding first, the arc of TIG preheats the metal later when the laser beam heat strikes the surface fumes form immediately so that the keyhole formation can happen to a greater depth for the same heat intensity; as both heat sources are incident on a single weld pool with a time lag for the formation of joints. The welding simulation models of similar and dissimilar materials for laser and arc welding processes are established and discussed by Tan et al. [5]. Kaplan [6] has given the theoretical basis of keyhole formulation.

The required parameters for deep penetration of beam so that more thick metal pieces can be joined. Different forms of heat volume shapes and energy distribution is discussed by Akella et al. [7]. Vemanaboina et al. [8] applied the thermally varying parameters for obtaining the temperatures distribution, obtained the structural effects of distortions, and induced residual stress in the welding process using the ANSYS package. The three-dimensional model of welding was developed to analyse and evaluate dissimilar metal joining. The resulting temperatures, deformations, and stresses were mapped for SS304 to Copper materials joining discussed by Akella et al. [9].

Padmanabham et. al [10] reports that hybrid MIG and laser welding process for higher thickness of mild steel plates were successfully obtained in single pass using CO_2 laser could weld for 12 mm mild steel plates with single pass welding using 3.5 KW with feed rate of 26 mm/s with V-groove and root face of 2.5 mm and root gap of 2 mm. Figure 1 is a typical hybrid laser and GMA (Gas Metal Arc) being applied simultaneously. It can be seen that laser beam vaporises the metal to form plasma cloud of metal vapour, keyhole formation, while the arc and filler rod are filling the root gap and forming the weld seam, a continuous joining to greater depths a benefit of double process joining.

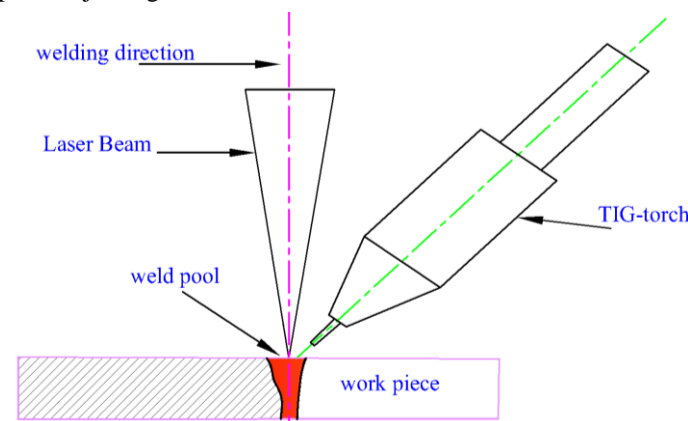


Fig. 1. TIG assisted laser-welding process.

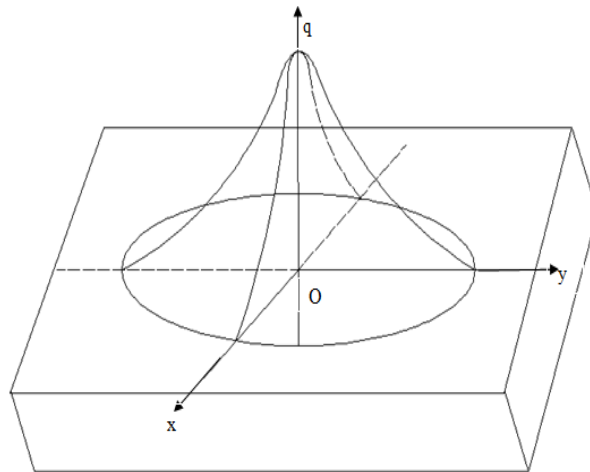
Subhashini et al. [11] reported MIG laser welding of maraging steel. Kong and Kovacevic [12] modelled with finite elements the lap joint of the Hybrid welding process. As a welding process will involve the transient thermal and couple the thermal output to structural analysis for estimation of temperature, distortion, and distributions in the weldment; Zeng et al. [13] provided the numerical simulation of magnesium alloy to steel, hybrid TIG-laser and experimentally validated. Finally, Qi and Song [14] gave the effect of providing interlayer metal in the TIG-laser welding process to obtain structural strength apart from obtaining a neat joint.

The challenge in the experimental measurement of temperature and keyhole fluctuation makes understanding very difficult expensive and time-consuming. Simulation is helpful to measure the parametric estimation by considering the known material properties, geometry and weld bead shape. Models need more assumptions due to the complexity of process understanding and implementation of molten and plasma vapour phase temperature estimation. FEM is one of the typical tools, which make estimating the thermal and residual stress analysis with some limitations with the physical assumptions.

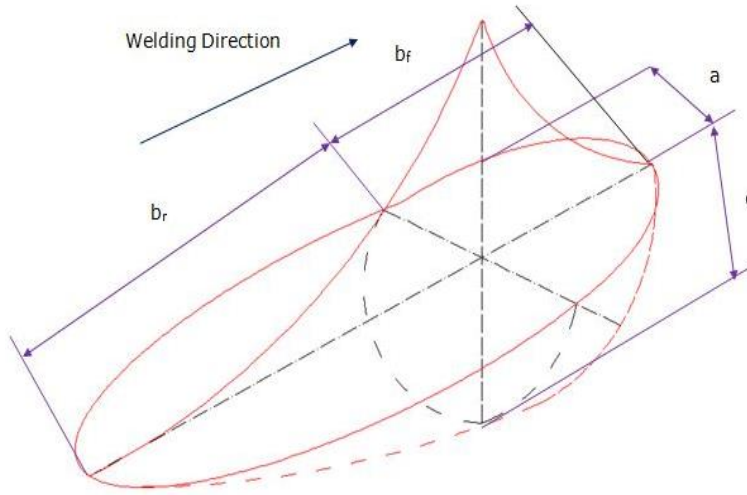
In this study, the total heat of the welding is distributed first to the surface heat, which represents the TIG process. The remaining portion of the heat is due to the laser beam, which happens to provide lateral heat to the joining metal pieces. This work mainly emphasis on a thermal response from the hybrid welding process on the residual stress using Finite Element Analysis. ANSYS software was used for modelling the welding process with thermal parameters and the output was obtained in 3D range.

2.Simulation Formulation

The present work incorporates transient thermal analysis first and later coupled to the structural analysis using ANSYS software. The Solid-70 element is used for the 3D thermal analysis, which incorporates the heat load in the designed shape and value, the boundary conditions of conductive, convective and radiation in nature. The output temperature distribution, in an uncoupled formulation, is transferred to the structural model, where 3D elements of Solid-45 are used. The structural loads of boundary conditions of clamping are incorporated, and the results of structural distortion and stresses are obtained. Again, the temperature dependent parameters of structural properties are used here. In Figs. 2 (a) and (b) the double Gaussian and double ellipsoidal heat source model were generally well for laser and arc welding processes proposed by Goladk et al. [15], for 3-D numerical welding simulation model for laser and arc welding process.



(a) Gaussian distribution in the mid-surface.



(b) Double ellipsoidal heat flux.

Fig. 2. Heat flux for laser and arc welding process.

The governing equation of combined laser and arc energy conservation is shown in Eq. (1):

$$\frac{\partial(\rho cT)}{\partial t} = \frac{\partial^2(k_m T)}{\partial x^2} + \frac{\partial^2(k_m T)}{\partial y^2} + \frac{\partial^2(k_m T)}{\partial z^2} + q_{laser}(x, y, z, t) \tag{1}$$

where t is the time, ρ is material density, c is the specific heat of material, and k_m is thermal conductivity or double ellipsoid, with a, b, c as semi-axes in 3-directions.

$$Q(x, y, z) = \frac{6\sqrt{3}r_f Q}{abc\pi\sqrt{\pi}} \exp\left(-\frac{3x^2}{c^2_{hf}} - \frac{3y^2}{a^2_h} - \frac{3z^2}{b^2_h}\right) \tag{2}$$

Eq. (2) gives this ellipsoid heat, which is mostly used for shallow or less dense distribution as in the conduction mode, used in MIG or TIG processes. The laser heat is entrapped in the keyhole and is defined uniformly on the lateral joining surfaces.

Radiation is a fourth order equation in T and would be causing nonlinearity in the formulation. Whereas, convection is linear in a variation of temperature T . Eq. (3) represents the combined heat convective transfer coefficient (H):

$$H = 24.1 * 10^{-4} \varepsilon T^{1.61} \tag{3}$$

This value of convective heat transfer is used in modelling which is acceptable to ANSYS and would incorporate the effects of convection and radiation. If q_L (W/m^2) is the heat flux of laser and q_T (W/m^2) is the heat flux of TIG process, then the total flux q is a linear combination of the above two given as Eq. (4):

$$q = q_L + q_T \tag{4}$$

3. Thermal Analysis

The weld geometry is carried out using ANSYS. The model is developed using the APDL and meshing of the model by tetrahedron is shown in Fig. 3. One-half of the symmetric two pieces to be welded. The length of the part and hence welding seam length is 420 mm width is 150 mm and thickness are 3 mm. Thermal properties of SS316L i.e. conductivity, specific heat, density is temperature dependent are used for in the simulation process. The temperature dependent thermal conductivity properties are shown in Fig. 4(a) the thermal conductivity increases with temperature and (b) the density is found to decrease with increase in temperature and specific heat is increasing with increase in temperature.

The appropriate proportions of ellipsoidal heat source were applied on the surface of the metal along the length direction for the transient thermal analysis. The laser heat is applied on the lateral face of thickness below the surface. Thermal load steps are increased up to time=1000 s to allow the weldment cool down to ambient temperature for the physical joints. The temperature distribution was evaluated at various zones on the surface of the model and thickness of the weldment. A time increment of $\Delta t = 0.1s$ was used. The weld starts with all the surface heat, given as input on the surface of weld region.

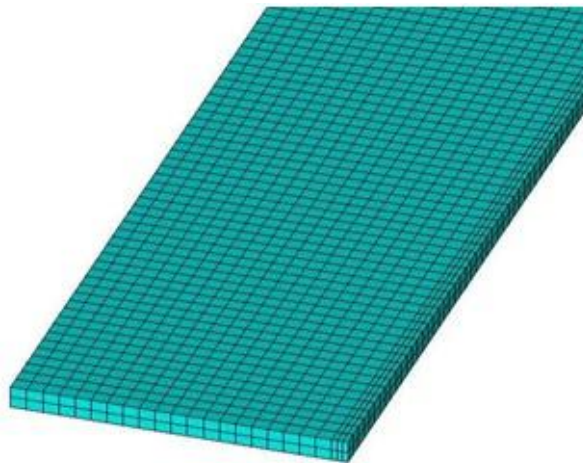
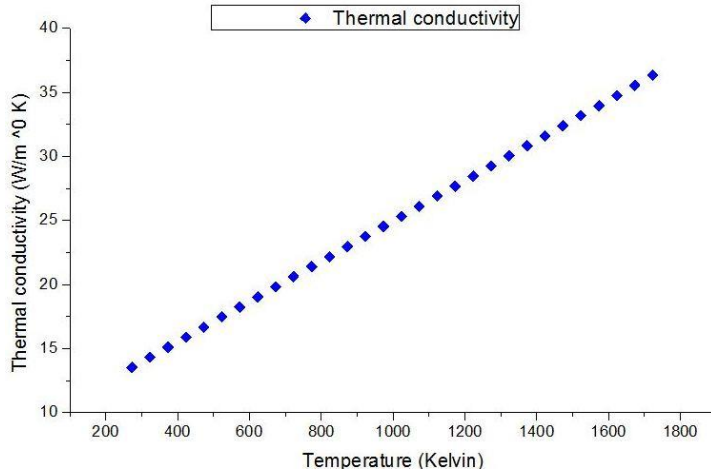
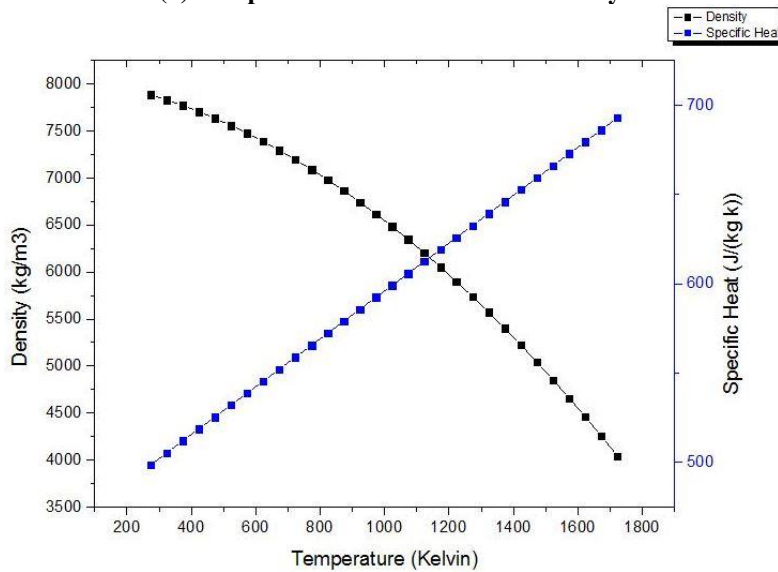


Fig. 3. Meshed model.

Figure 5 shows the colour code of temperature, in Kelvin, distribution along the weld length after both heat fluxes act on the metal is shown. The colour representation of temperature distribution consists of the fusion zone in red colour, HAZ is yellow and the rest is in blue colour over the base plate. Transient thermal analysis of temperature is done for 1000 seconds to allow the material to reach ambient temperature. Figure 6 shows the 3D temperature distribution of the weldment after 7.12 s, melting can happen up to yellow region, fusion zone. It is also seen that temperature has not reached above ambient, 300 K at the blue zone of edges. Three models were made, first full two plates with all power on the surface. Next, a symmetric half plate with half the power on the surface and finally, a half plate with half power lateral along thickness. These models can be representing surface conduction models on the surface and the lateral heat conduction as in keyhole model.



(a) Temperature vs thermal conductivity.



(b) Temperature vs. density and specific heat.

Fig. 4. Temperature dependent properties.

Figure 6 shows the distribution in the finite element model. The maximum temperature is at the weld bead area of 2528 K and the temperature lowers away from the weld bead, with a minimum temperature of 303 K, where the base plate is at ambient temperature. The temperature change, shown in Fig. 7. along the weld width, lateral to the weld direction gives an indication of fall of temperature from Fusion zone, to HAZ and to the base plate. Temperature variation along the thickness is shown in Fig. 8. varies from a maximum at the top where surface heat flux is given to ambient temperate at the bottom. Also, it is observed that there is an inflexion, change in slope at 1.5 mm. This could be due to the end of surface heat affect o the TIG Process.



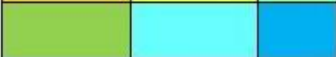

Colour Indication Of The Temperature	Description
	Max Temperature Distribution
	Weld Pool Temperature
	Heat Affected Zone
	Less Affected Or Unaffected Zone

Fig. 5. Colour indication of the temperatures in model.

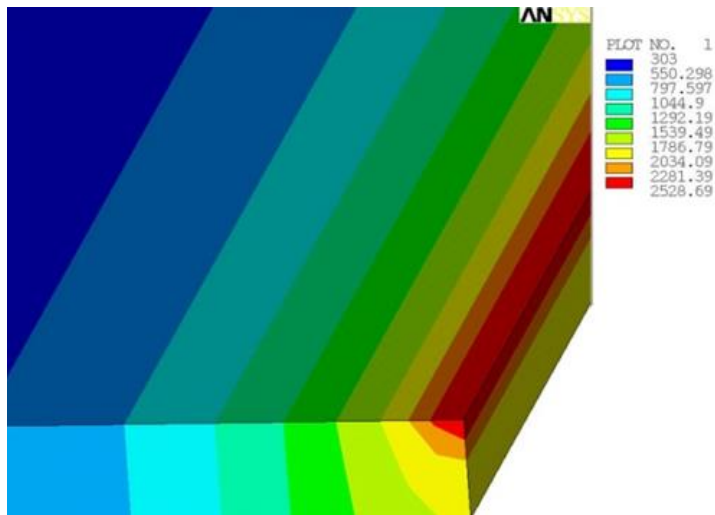


Fig. 6. Temperature distribution in the weldment.

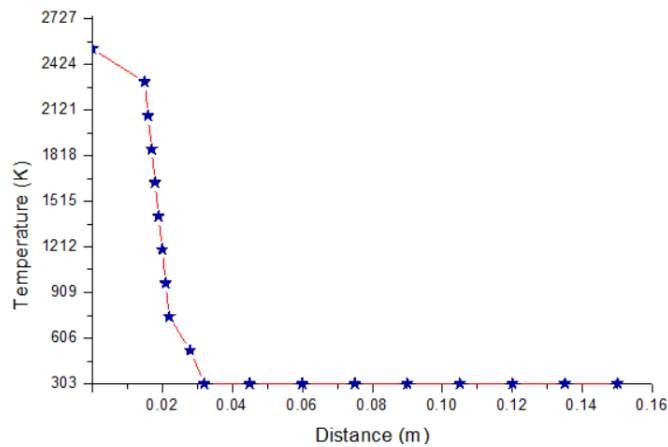


Fig. 7. Temperature distributions along weld.

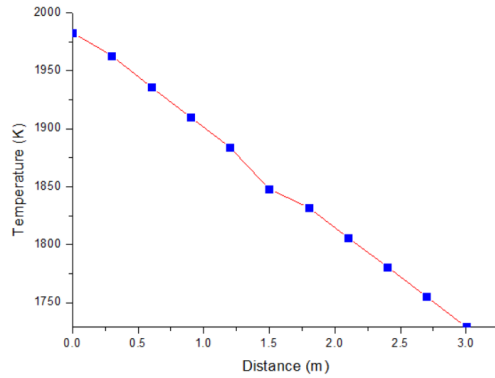


Fig. 8. Temperature distributions in depth.

4. Structural Analysis

The temperature distribution of thermal model is transferred to the structural model in a sequentially coupled analysis. Once the temperature load is given, the edge opposite the weld edge is clamped as a boundary condition. After the analysis output of stresses and distortion are obtained which can be modelled. The stress is due to metal melting and phase transformation and remains as residual stress as shown in Fig. 9. As the welding process has been carried out in the longitudinal direction, the metal tends to expand near the fusion zone. The temperature gradient is giving to decrease as moving towards the transverse direction, expresses the compressive stress as a result of mechanical, thermal and boundary conditions chosen, in order to compensate for the expansion occurring at the weld zone. It has been clearly seen from the Fig. 9, which the edges of the plate in the transverse direction experiencing compressive stress varied from -85 MPa to 18.2 MPa. The value at the welded portion, which a maximum is 18.3 MPa and is within the yield stress of 240 MPa with a factor of safety about 13.11. Residual stress estimate is important for failure and structural reliability. A second factor of importance in structural stability and for fitment with other parts is deformation and distortion. The residual stress is seemed to be occurring at the edges and is quite uniform along the length as seen in Fig. 10.

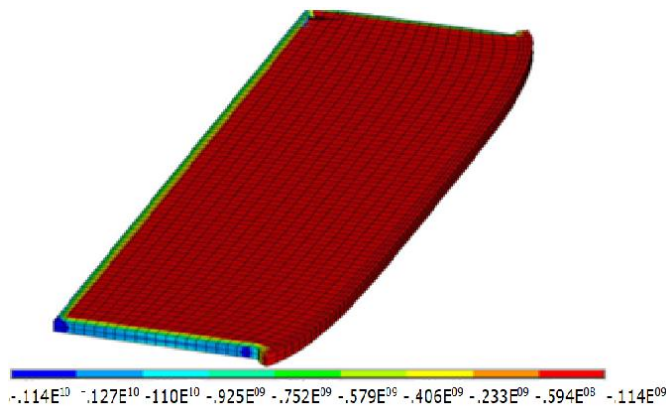


Fig. 9. Residual stresses in the weldment.

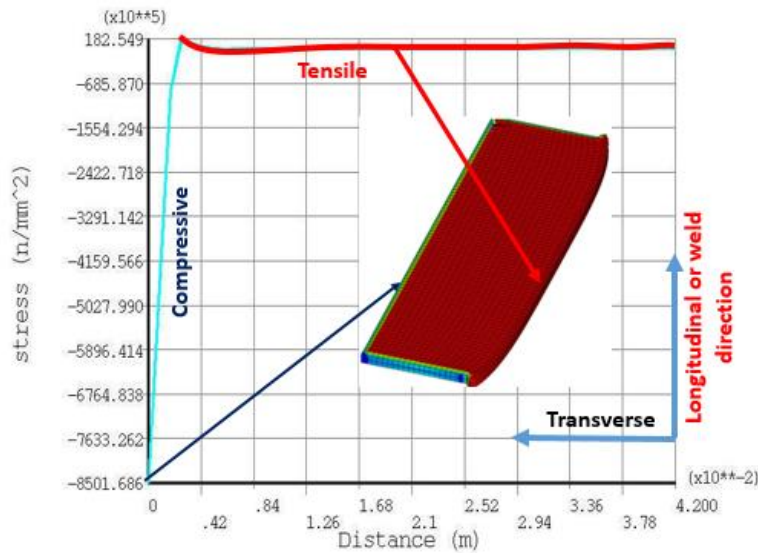


Fig. 10. Residual stresses distribution from the base plate to fusion zone in the transverse direction.

5. Conclusions

An FEA of Hybrid TIG-Laser is modelled. Simulation results of thermal and stress analysis indicate the typical temperature range in FZ and HAZ. Along weld line, it indicates similar profile constantly both in temperature and distortion. Hybrid laser with Keyhole mode analysis indicates temperatures 2528 K and stress levels of 18.3 MPa. Temperature distribution having 1600 K to 2528 K is 0.01 m only which constitutes the fusion zone, heat-affected zone is 0.01 m to 0.02 m. Where the temperature reduces to 500 K. Rest of the area constitutes base material. The stress distribution throughout is having a good factor of safety 13.11.

References

1. Shah, B.; and Madhvani, B. (2017). A review paper on a-TIG welding process. *International Journal of Science Technology & Engineering*, 3(9), 312-315.
2. Sándor, T., and Dobránszky, J. (2007). The experiences of activated tungsten inert gas (ATIG) welding applied on 1.4301 type stainless steel plates. *Materials Science Forum*, 537-538, 63-70.
3. You, D.Y., Gao, X.D., and Katayama, S. (2013). Review of laser welding monitoring. *Science and Technology of Welding and Joining*, 19(3), 181-201.
4. Belhadj, A., Bessrou, J., Masse, J.-E., Bouhaf, M., and Barrallier, L. (2010). Finite element simulation of magnesium alloys laser beam welding. *Journal of Materials Processing Technology*, 210(9), 1131-1137.
5. Tan, W.; Bailey, N.S.; and Shin, Y.C. (2013). Investigation of keyhole plume and molten pool based on a three-dimensional dynamic model with sharp interface formulation. *Journal of Physics D: Applied Physics*, 46(5), 055501.

6. Kaplan, A. (1994). A model of deep penetration laser welding based on calculation of the keyhole profile. *Journal of Physics D: Applied Physics*, 27(9), 1805-1814.
7. Akella, S.; Vemanaboina, H.; and Buddu, R.K. (2016). Heat flux for welding processes: model for laser weld. *Sreyas International Journal of Scientists and Technocrats*, 1(1), 10-15.
8. Vemanaboina, H.; Akella, S.; and Buddu, R.K. (2014). Welding process simulation model for temperature and residual stress analysis. *Procedia Materials Science*, 6, 1539-1546.
9. Akella, S.; Harinadh, V.; Krishna, Y.; and Buddu, R.K. (2014). A welding simulation of dissimilar materials SS304 and copper. *Procedia Materials Science*, 5, 2440-2449.
10. Padmanabham, G.; Shanmugarajan, B.; and Prabhakar, K.V.P. (2012). Laser MIG hybrid welding of thick plates of mild steel in single pass. *Indian Welding Journal*, 45(2), 29-39.
11. Subashini, L.; Phani Prabhakar, K.V.P.; Padmanabham, G. (2014). Laser MIG hybrid welding of maraging steel. *Proceedings of the Conference of Metallurgists (COM)*, Vancouver, Canada.
12. Kong, F.; and Kovacevic, R. (2010). 3D finite element modeling of the thermally induced residual stress in the hybrid laser/arc welding of lap joint. *Journal of Materials Processing Technology*, 210(6-7), 941-950.
13. Zeng, Z.; Li, X.; Miao, Y.; Wu, G.; and Zhao, Z. (2011). Numerical and experiment analysis of residual stress on magnesium alloy and steel butt joint by hybrid laser-TIG welding. *Computational Materials Science*, 50(5), 1763-1769.
14. Qi, X.; and Song, G. (2010). Interfacial structure of the joints between magnesium alloy and mild steel with nickel as interlayer by hybrid laser-TIG welding. *Materials and Design*, 31(1), 605-609.
15. Goladk, J.; Chakravarti, A.; and Bibby, M. (1984). A new finite element model for welding heat sources. *Metallurgical Transactions B*, 15(2), 299-305.